JOURNAL OF APPLIED ELECTROCHEMISTRY 19 (1989) 668–676

Measurement of bubble nucleation rates by an acoustic method*

S. D. LUBETKIN

University of Bristol, Department of Physical Chemistry, Bristol BS8 1TS, UK

Received 25 July 1988; revised 1 September 1988

Bubbles which form at the surface clearly affect the efficiency of electrodes during their residence. The residence time is related to the detachment rate, and the surface density of bubbles is strongly affected by the nucleation rate. A new acoustic technique for detecting the bursting of bubbles at a free liquid surface, and hence for measuring bubble nucleation rates, is reported here. In suitable circumstances, the number of bursts is closely correlated with the number of bubbles actually nucleating, and this has allowed a testing of theoretical equations [1] for the heterogeneous nucleation of bubbles on various surfaces. It is pointed out, however, that the description of the mechanism implicit in the derivation of the equations referred to in [1] may not be correct, and that there is good reason for believing that it will not in general be applicable for calculating bubble hetero-nucleation rates.

Nomenclature

θ	contact angle: θ_r is receding angle, θ_a is advancing angle
α	saturation ratio: $\alpha = \sigma + 1$
β	half-angle of a conical pit
γ	interfacial tension
σ	supersaturation: $\sigma = \alpha - 1$
P	pressure: P_v vapour pressure, P_l pressure in liquid
τ	characteristic time: τ_d detachment time: τ_n nucleation time
J	rate of nucleation
Ω	molecular volume
k	Boltzmann constant
T	absolute temperature
B, B'	pre-exponential constants in nucleation equations
Γ	surface excess, adsorbed amount
R	gas constant
$\mathscr{L}$	dimensionless ratio between detachment and nucleation times
$\mathscr{N}$	number of molecules per unit volume in active sites
N	number of molecules per unit volume of solvent

1. Introduction

There have been several papers over the last quarter of a century or so which have dealt with the kinetics of bubble nucleation, some of them drawing the close analogy between the kinetics of evolution of dissolved gases and the similar phenomenon of boiling in a single component system [2–5], and others, much earlier, which dealt with the evolution of CO_2 from various aqueous solutions containing other components in a more qualitative way [6].

When the nucleation is truly homogeneous, and thus occurs in the bulk mother phase where the influence of any interface in the system is negligible, it is expected that the equations developed in [1–5] will apply, albeit with some modification (see section 4). In the much more usual case where the nucleation is heterogeneous, and therefore takes place for example on the surface of the containing vessel, or at an electrode, the equations will often be seriously in error.

The practical implication of the argument to be presented here is that on the surface of an electrode, for example, the overall kinetics of bubble release may not be governed by the rate of nucleation alone: the rate of detachment, generally ignored in previous treatments, may be slow, and hence may become the rate-determining step. The conditions required to make the surface catalytic for the nucleation of bubbles, as elaborated in refs [1–5] and elsewhere, are exactly the conditions required to make detachment of the bubbles once formed, difficult. It appears that if the contact angle, θ, is large, thus favouring the formation of a critical sized bubble, then the bubble so formed will have difficulty in becoming detached from the surface. Naturally whilst the growing bubble is attached to the nucleation site, no further nucleation can take place there. On the other hand, if the contact angle is small or zero, then the nucleation event becomes more difficult, approaching the limiting case of homogeneous nucleation, as the contact angle approaches

* Paper presented at the 2nd International Symposium on Electrolytic Bubbles organized jointly by the Electrochemical Technology Group of the Society of Chemical Industry and the Electrochemistry Group of the Royal Society of Chemistry and held at Imperial College, London, 31st May and 1st June 1988.

0021-891X/89 $03.00 + .12

zero. Since under identical conditions of supersaturation, the homogeneous nucleation rate will usually be many orders of magnitude slower than the heterogeneous rate, this alteration of mechanism may cause a very significant lowering of the overall rate of bubble release.

There are several difficulties involved in testing the equations in the literature relating to the nucleation of bubbles in liquids, and the method described here is applied to the special case of the CO_2/H_2O system nucleating on the walls of the stainless steel pressure vessel, or on glass. It is probably worth stating that the principles elaborated in this paper will be valid for electrogenerated bubbles as well as for bubbles formed from a supersaturated gas solution, although the experiments reported here apply only to the latter.

It is likely that this new experimental method will also work for other substrates and liquids which have a small value of the contact angle θ, but it is probable that substrates with large θ values will encounter the problems alluded to above, where detachment kinetics may dominate the overall rate of bubble release.

Experimentally, the four most important independent variables in the equation of Wilt [1] are: (i) the saturation ratio, α; (ii) the contact angle, θ of the three-phase contact line between solution, gas bubble and the nucleation site; (iii) the half-angle of the conical pit, β, which is expected to be the preferred site for heterogeneous nucleation; (iv) the interfacial tension, γ, between the liquid and vapour phases. For a proper test of the theory, the temperature, T, and the pressure, P, must also be controlled. In this paper, an experiment is described in which four of these variables, α, θ, P and β, were deliberately altered, and the effects on the kinetics of bubble nucleation from a supersaturated solution of CO_2 in water were then measured.

2. Experimental details

2.1. *Apparatus*

The apparatus consisted of the following. (1) A stainless steel pressure vessel, with a glass window let into the top for observation of the nucleation, growth and detachment of the bubbles. The vessel had an outer jacket through which thermostatically controlled water could be pumped, to maintain a known and constant temperature in the pressure vessel. It was possible to fit a glass liner into the pressure vessel internally, so that a glass surface could be examined for its nucleation behaviour. (2) The pipework and pressure gauges, and the cylinder of analytical grade CO_2. (3) The computer and associated electronic components.

The source of CO_2 was a cylinder of analytical grade gas (Distillers Co. Ltd) which was connected by a reducing valve to the pipework leading to the pressure vessel. A sensitive pressure transducer (Sensortec GmbH) was incorporated in the pipework, and was capable of resolving to 1 part in 10^5. As a visual check

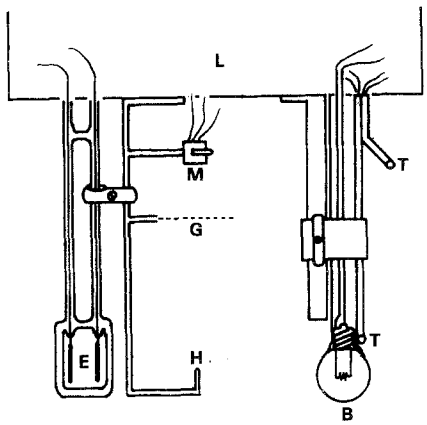

Fig. 1. Showing the microphone (M), stainless steel gauze (G), conductivity electrodes (E), low power light bulb (B), the thermistors (T) and the nucleation site holder (H), all attached to the lid of the pressure vessel (L).

on the correct operation of the pressure transducer, two mechanical gauges were also incorporated in the gas circuit, and these had the added advantage of allowing for manual operation of the complete system, should this be desired. The gauges were isolated from the main gas pipe by an electromagnetic valve, which was controlled from the computer, and further valves isolated the needle-valve which controlled the escape of gas to the atmosphere, and the cylinder itself.

A BBC model 'B' microcomputer normally contolled the sequential operation of the valves, the reading of the pressure transducer, temperature, and most important, the counting of the bubble bursts, as detected by the microphone and its amplifying circuitry.

The components inside the pressure vessel are shown in Fig. 1, and comprised: (1) a pair of platinum electrodes used to measure the conductivity of the carbonic acid in its dissociated form; (2) a sensitive electret microphone mounted with a sheet of fine stainless steel gauze below it to protect if from splashing by droplets formed by the bursting bubbles; (3) a pair of matched thermistors, one placed in the gas phase above the solution, and the other dipping into the solution; (4) a magnetic stirrer, driven by an external motorized magnet; (5) a low power light bulb to illuminate the inside of the vessel; (6) a bent stainless steel wire, positioned immediately below the microphone, which was used to hold the specially prepared surfaces with their known geometry nucleation sites (see Section 2.2.2).

The electrical connections to these devices were via a feedthrough in the lid of the vessel, the lid being held to the body of the pressure vessel by stainless steel bolts, and sealed with a Viton A 'O' ring.

2.2. *Nucleation sites*

A variety of nucleation sites have been examined, and some preliminary results for the hetero-nucleation of bubbles on the stainless steel walls of the pressure vessel have been reported [7]. Further results for stainless steel are given below, but the main results relating to this paper are for (1) glass, and (2) CR39, a poly-

(carbonate) polymer surface, these two materials being chosen since, *inter alia*, they have low and high contact angles, respectively, and thus are expected to correspond to the extremes of behaviour referred to in Section 1.

2.2.1. Glass surface. The glass liner of the pressure vessel was cleaned in aqua regia, then washed sequentially with copious quantities of single and double distilled water. It is known from other experiments that this treatment leaches small amounts of basic components from the glass, and that this leaves the glass surface modified in such a way as to promote the nucleation of crystals from the vapour [8]. It was therefore of some interest to find out if this treatment also promoted the nucleation of bubbles.

2.2.2. CR39. CR39 is a poly(carbonate) polymer, used commercially to detect the presence of ionizing radiation [9], which it does as a result of the chemical damage done to the polymer by the passage of alpha particles or other charged radioactive decay fragments. This damage is revealed by attacking the polymer with 6.25 M NaOH solution at elevated temperatures, whereupon the track of the alpha particle opens up into a conical pit, the half-angle, β, of which is governed by several factors. The chief factors are the energy of the alpha particle and the bulk etch rate of the polymer, which itself varies according to how old the sample of polymer is, and the temperature at which the etching is carried out. By choosing an appropriate alpha source (in these experiments, americium, $_{95}Am^{241}$, with a mean alpha energy of about 5.5 MeV) the pits could be designed to have half-angles in the range expected to be good heterogeneous nucleation sites, β lying roughly between 2 and 5°, when the temperature of etching was 85° C.

The three-phase contact angle on this polymeric material could be varied by treating the surface with chlorotrimethyl silane, which bonds to the polymer, and produces a surface covered with methyl groups, thus increasing the degree of hydrophobicity of the surface. The contact angle at the three-phase line was determined by both the sessile drop method, and by directly measuring the contact angle, θ, of a bubble blown onto the polymer surface under water. The results for the latter method are shown below, in Section 3.5.

The pieces of treated polymer were attached to a glass microscope slide, and this was then placed in the pressure vessel.

2.2.3. Stainless steel. The base of the stainless steel pressure vessel was polished carefully with diamond

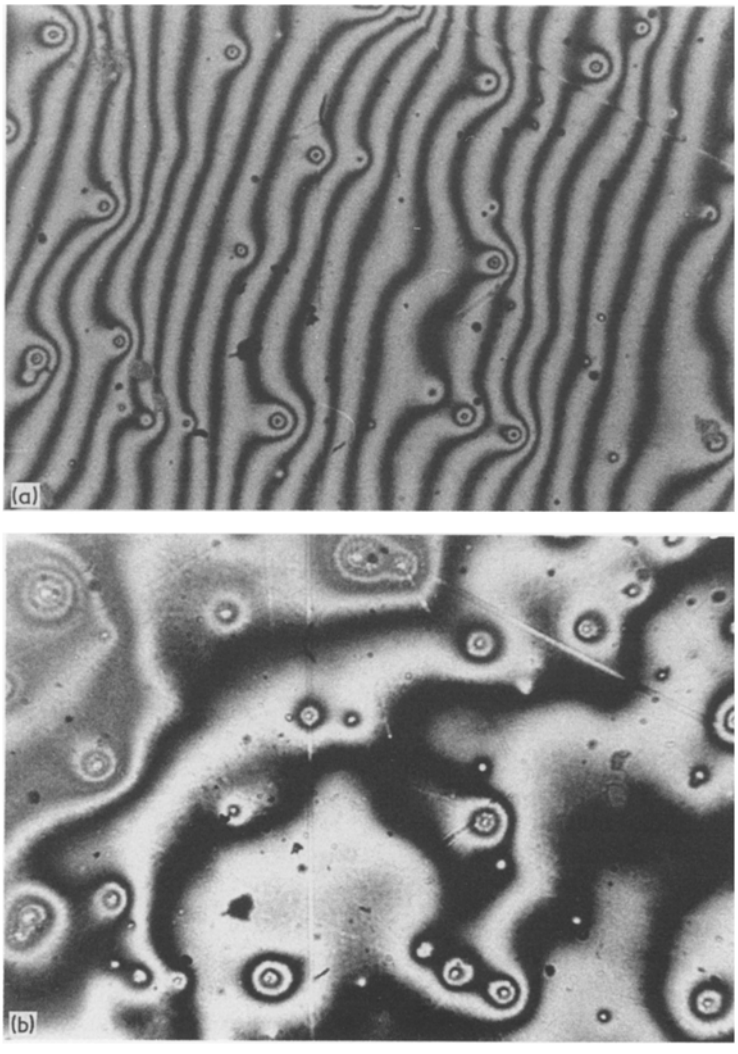

Fig. 2. Monochromatic (a) and white light (b) interference photomicrographs of the same area of the polished stainless steel surface of the pressure vessel. The conical pits and typical scratches are clearly visible.

pastes of decreasing size, and then lapped. The surface finish was then inspected with an optical interference technique. The interference micrographs, Figs 2a and 2b, showed that most of the detectable sites were roughly conical and about 1.5 μm in size, although there were also some scratches, about 1 μm in width but up to a few mm in length.

2.3. *Method*

With either the bare stainless steel vessel walls, the glass liner or a chosen nucleation site in position, and the pressure vessel about two-thirds filled with doubly distilled water, the required pressure of CO_2 was applied, stirring commenced, and the conductivity was monitored. When the solution was saturated, as judged by a steady reading of the conductivity – a process which could be quite slow [7] – the pressure vessel was isolated by means of the electromagnetic valve from the cylinder. The pressure was then released to the target pressure via the needle valve, at an appropriately slow rate, to avoid damaging the microphone.

There are two obvious ways of conducting these experiments, these being (1) to release the pressure to the target value, and then control the electromagnetic valves to hold the pressure constant at that value, or (2) to release the pressure to the target value, and then close the system completely, so that the bubbles as they burst gradually cause an increase in pressure in the vessel. Each method has its advantages, but the second is preferred since the rising pressure, as monitored by the pressure transducer, gives an independent check on the bubble count (see Section 4.3).

The number of bubbles released and the increase in pressure were monitored with time, as was the conductivity of the solution, and the results were automatically stored in the computer.

3. Results

3.1. *Acoustics of bubble bursts*

The microphone used in these experiments had a dynamic range of approximately 50 Hz to 16 kHz. It is expected that some parts of the acoustic event associated with the bubble burst have higher frequencies than the upper limit of the microphone used, so that the data are probably incomplete. However, it is an easily established fact that there are at least some frequencies associated with the burst in the audio range of normal human hearing, i.e. close to the range for this microphone.

The acoustics of a typical bursting event are shown in Fig. 3a demonstrating the characteristic features of a fast rise time (a ⇒ b) followed by an approximately exponential decay, or tail (b ⇒ c) which showed some periodicity but not always of a regular kind. Many such bursts were examined, and these general features were found to be characteristic. The frequencies

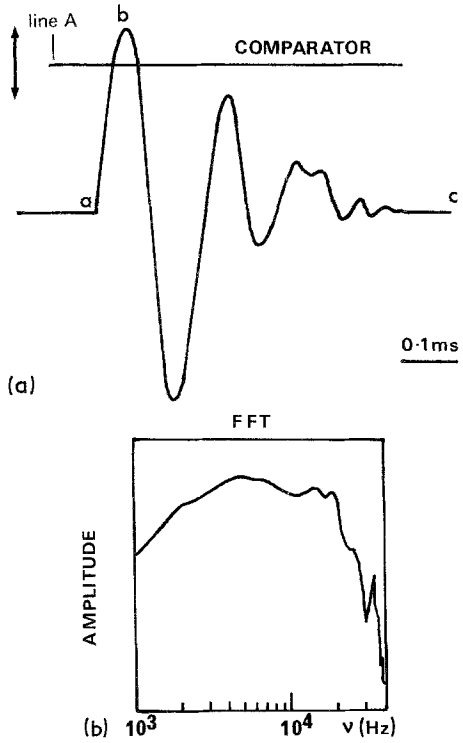

Fig. 3. (a) The acoustics of a typical bursting event, demonstrating the characteristic features of a fast rise time (a ⇒ b) followed by an approximately exponential decay, or tail, (b ⇒ c). The horizontal line A shows the (variable) position of the comparator level. (b) The FFT of a typcial bursting event.

present were analysed by fast Fourier transform (FFT) techniques, and a typical FFT spectrum is shown in Fig. 3b, revealing a rather broad band of frequencies, without any very characteristic peak. For this reason, the original intention, which was to detect the bubble by a characteristic frequency, was abandoned, and the burst was detected by using the sharply rising part of the original signal (a ⇒ b in Fig 3a). The amplifier circuit had built into it a set of filters chosen to make it sensitive to the positive-going edge of the amplified signal, and a variable comparator, the setting of which decided the amplitude level at which a burst was detected. The comparator level was chosen so that the primary peak of the bursting event initiated the count, but the secondary peaks fell below the comparator voltage setting, as shown in Fig. 3a. The software in the computer had a built-in but variable delay time during which no further bursts were recorded, to avoid counting the peaks in the tail (b ⇒ c in Fig. 3a) as further bursts. This was necessary, since the amplitudes of both the primary and secondary peaks depended on a number of factors, including the distance of the burst from the microphone, and there was in general no unique setting of the comparator which eliminated all the secondary peaks whilst at the same time retaining all the primary peaks. This imposition of a dead-time is completely analogous to the procedure needed in photon counting, or with Geiger tubes [10]. The software delay limited the maximum rate at which bubbles could be detected to about 500 s^{-1}, and this in turn limited the maximum supersaturation and thus the bursting rate, under any given set of conditions.

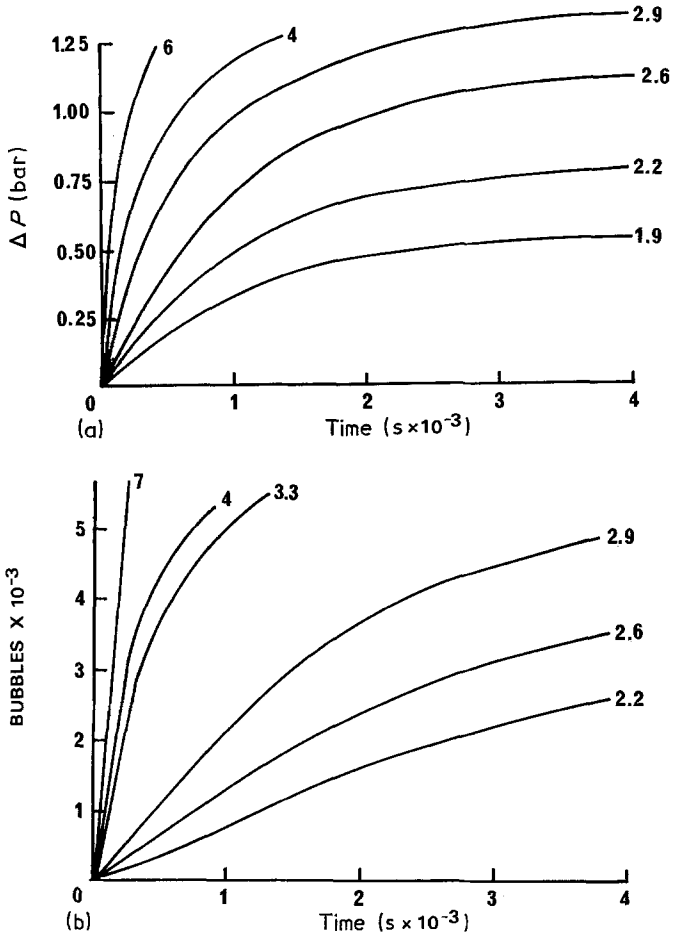

Fig. 4. The raw data for the pressure rise (a), and the number of bubbles bursting as a function of time after the solution became supersaturated (b), on a stainless steel surface, for various values of α. Not all the data are shown in either figure.

3.2. *Rate of nucleation on stainless steel*

The results of a set of experiments performed on the stainless steel walls of the pressure vessel are shown in Figs 4a and 4b. In Fig. 4b are shown the numbers of bubbles bursting as a function of time for a set of supersaturations between 8 and about 2, and at a temperature of 25° C. For a kinetic analysis, the initial rate of bursting must be used, since as bubbles form, rise and burst, the supersaturation is altering, and whilst this introduces very small errors at short times after the imposition of the supersaturation, this error

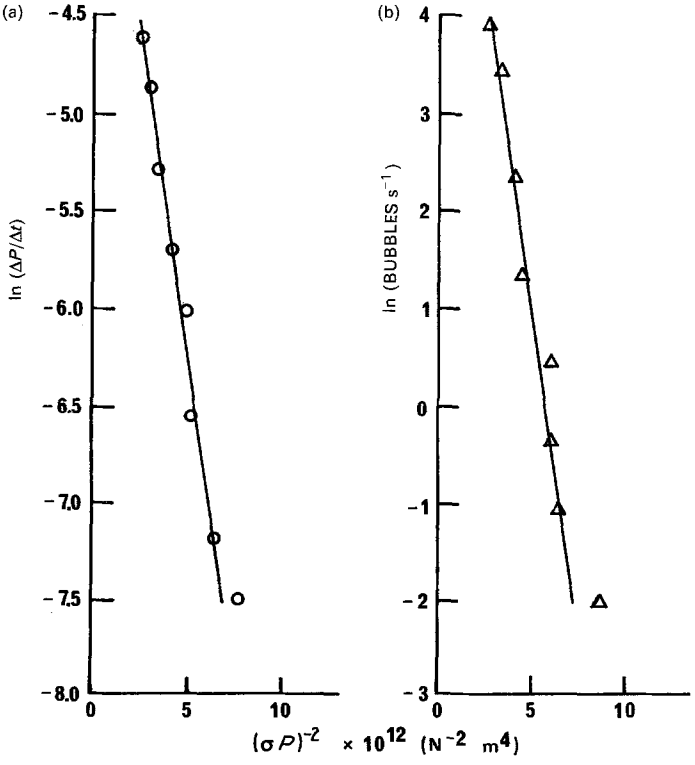

Fig. 5. The nucleation data from Fig. 4 for the stainless steel surface, plotted according to Equation 7. In (a), it is the rate of pressure rise that is used, whilst in (b), the ordinate is obtained from the rate of bubble bursts.

increases with time. In Fig. 4a, the results for the pressure rise corresponding to the same experiments as in Fig. 4b are plotted.

A somewhat simplified version of the equation from [1] is used to plot these experimental data, as shown in Figs 5a and 5b. The abscissae in each case are the same, and correspond to $(\sigma P)^{-2}$, whilst the ordinate in each graph is different: in Fig. 5b it is the natural logarithm of the initial bubble rate, whilst in Fig. 5a it is the natural logarithm of the initial pressure rise rate from the same experiment. A comparison of the two graphs serves to show how well the two sets of data agree: this demonstrates that the bubble counting and the pressure rise method give essentially the same information in this case.

3.3. *Nucleation on CR39*

Samples of CR39 which had been exposed to alpha radiation damage and subsequently etched to produce conical pits were then tested for their properties as nucleating surfaces. The conditions used during the exposure to radiation and subsequent etching were such as to give a range of half-angles of the cones lying roughly between 2 and 5°.

These experiments gave results which were unexpected. The rates of nucleation, judged by the number of bubble bursts and by the pressure rise data, were very small, despite the fact that the measured contact angles, θ, on the treated polymer surface were about 112° for the advancing angle and about 85° for the receding angle — a range which was expected to provide very favourable conditions for nucleation in the conical sites with the supersaturations used.

Careful observation revealed that the bubbles did not readily detach from the polymer surface, and were thus shielding bubble nucleation at these potential nucleation sites, and that the bubbles reached quite large sizes before detachment, growing over adjacent nucleation sites and also blocking nucleation there.

3.4. *Glass surfaces*

The rate of nucleation was measured with the glass liner fitted inside the stainless steel pressure vessel. The results of measurements made in this way are plotted in Fig. 6 as the logarithm of the initial rate of pressure rise against the same abscissa, $(\sigma P)^{-2}$ as before. The agreement between the results on stainless steel (Fig. 5) and these results on glass is good.

3.5. *Contact angles*

The contact angles of a saturated CO_2 solution on the various surfaces used for nucleation were measured by both the sessile drop and bubble contact methods, and the values for the bubble method are summarized in Table 1.

Because of the intrinsic instability of the chlorotrimethyl silane on the polymer surface towards hydrolysis, the contact angle decreases with increasing time of exposure to water, and this decrease is faster still when the modifed polymer surface is in contact with carbonic acid solutions.

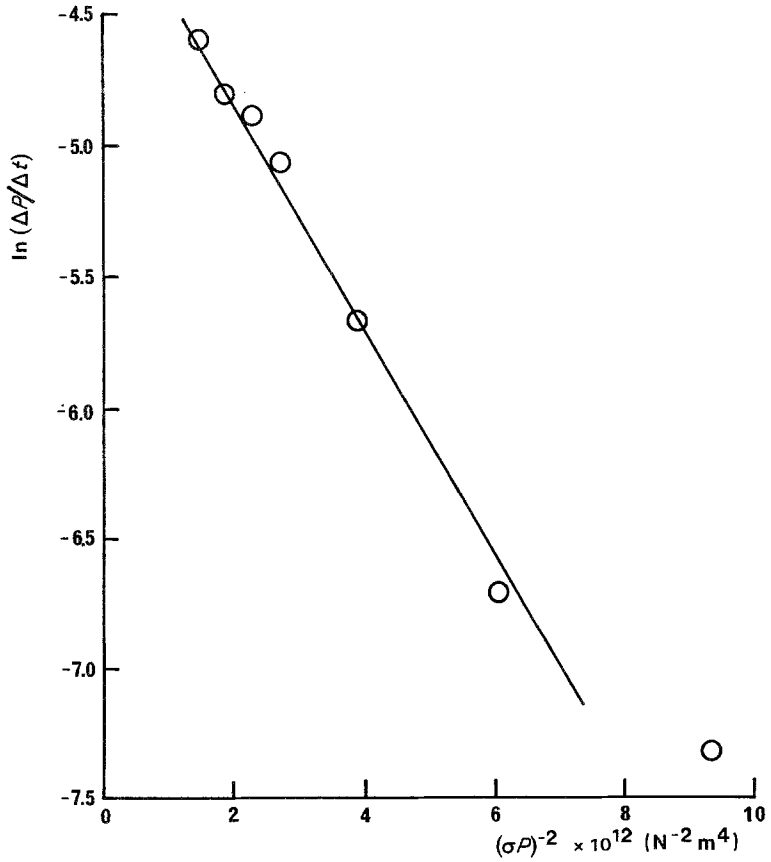

Fig. 6. The rate of nucleation on the glass liner of the pressure vessel, as measured by the rate of pressure rise.

Table 1. Advancing and receding contact angles on various surfaces

		Advancing (θ_a)	*Receding* (θ_r)
(1) Glass		0 ± 5°	0 ± 5°
(2) Steel		0 ± 5°	0 ± 5°
(3) CR39	Time (h)		
	0	112 ± 2°	85 ± 2°
	2	105 ± 2°	82 ± 2°
	17	100 ± 2°	76 ± 2°
	22	95 ± 2°	70 ± 2°
	46	90 ± 2°	67 ± 2°
	70	88 ± 2°	65 ± 2°

4. Theory

4.1. *Heterogeneous nucleation in CO_2/H_2O system*

For the case of bubbles nucleating heterogeneously on a flat solid surface, the catalytic activity of the substrate is such that surfaces with higher θ values will be the better catalysts. The equation derived by Wilt [1], relating the rate of nucleation, J, to the degree of supersaturation, α, and the interfacial tension, γ, is quoted below:

$$J = B \exp\left[\frac{-16\pi\gamma^3\phi(\theta)}{3kT(P\alpha + \eta P_v - P)^2}\right] \quad (1)$$

The pre-exponential factor, B, is here considered to be effectively constant. This approximation is justified in the relatively restricted range of the present experiments. The function $\phi(\theta)$ is related to the geometry of the captive bubble, and changes from 0 to 1 as θ ranges over values from 180 to 0°.

$$\phi(\theta) = [2 + 3\cos(\theta) - \cos^2(\theta)]/4 \quad (2)$$

The undefined symbols in Equation 1 are P, the pressure, and η, a factor which in the present case is unity, but in the general case is defined as:

$$\eta = \exp[\Omega(P_l - P_v)/kT - C_2'/C_1'] \quad (3)$$

where P_l and P_v are the pressures in the liquid and the pure solvent vapour pressure, respectively. C_2' and C_1' are the number of moles of solute per unit volume of solvent, and Ω is the molecular volume of the solvent.

The equation can be further modified to take into account other geometrical sites for nucleation, and the interested reader is referred to [1] for such details. In that reference, it is shown that of the geometries considered, the preferred sites for nucleation are expected to be conical pits and, on this basis, the equation becomes:

$$J = B' \exp\left[\frac{-16\pi\gamma^3 f'(\theta, \beta)}{3kT(P\alpha + \eta P_v - P)^2}\right] \quad (4)$$

where $f'(\theta, \beta)$ is defined by:

$$f'(\theta, \beta) = [2 - 2\sin(\theta - \beta) + \cos(\theta)\cos^2(\theta - \beta)/\sin(\beta)]/4$$

The expectation that conical cavities will be the preferred sites is based upon a comparison of only some of the simplest geometries. It may be that parallel-walled slits or cracks could actually be better sites than conical cavities, but such sites were not considered in [1]. It should be noted that this treatment also ignores several potentially important effects, and in particular, the total pressure in the bubble is made up of two partial pressures: that of the solvent and that of the solute, and this total pressure is a function of the curvature as given by the Laplace equation:

$$\Delta P = 2\gamma/R \quad (5)$$

Furthermore, the surface tension, γ, is itself a function of the surface excess amount, Γ_2, of solute (in this case CO_2) adsorbed at the liquid/vapour interface, as governed by the Gibbs adsorption isotherm:

$$\Gamma_2 = \frac{-P_2}{RT}\left[\frac{\partial\gamma}{\partial P_2}\right] \quad (6)$$

where the subscript 2 indicates the solute.

For these reasons, it was expected that no further loss of accuracy would be incurred in simplifying the full Equation 4, and accordingly, the data were treated with Equation 7 below:

$$J = B' \exp\left[\frac{-16\pi\gamma^3 f'(\theta, \beta)}{3kT(\sigma P)^2}\right] \quad (7)$$

where the substitution $\alpha - 1 = \sigma$ has been made, and the factor ηP_v has been neglected in comparison to P.

It is at this point that it becomes important to consider the pre-exponential factor, B', in Equations 4 and 7. In the usual treatment of heterogeneous nucleation, as exemplified by [1], B' is a function which contains, amongst other parameters, $N^{2/3}$, where N is the number of molecules per unit volume in the liquid. Using the factor $N^{2/3}$ is equivalent to the implicit assumption that the nucleation is equally probable at any site in the interface. Here this is not a valid assumption, since the conical pits are strongly preferred sites. It would, therefore, be more appropriate to use a factor $\mathcal{N}^{2/3}$, where $\mathcal{N}$ is now the number of molecules per unit volume in the active sites. It should be noted that $\mathcal{N}^{2/3}$ will be smaller than $N^{2/3}$ by a factor of at least 10^{-7} when the area for heterogeneous nucleation is restricted to the tips of the conical pits.

4.2. *Nucleation rate and bursting rate*

The number of bubbles nucleated and the number actually bursting at the free liquid surface are clearly related but the question is, what is the relation? If each bubble nucleated becomes instantly detached, rises to the surface and bursts without coalescing, then the number of bursts will equal the number of bubbles nucleated. Under the conditions which satisfy these criteria, some of which have been discussed elsewhere [7], the number of bursts detected can be related to the pressure rise in the closed system as follows.

It will be assumed that the bubbles are mono-sized, and that each therefore contains the same number of moles, n, of CO_2 gas (assumed to behave ideally). It is further assumed that the rate of loss of CO_2 from the solution by diffusion through the interface is small compared to the loss by bubble evolution into the closed head-space volume, v.

Thus:

$$\frac{\partial P}{\partial n} = \frac{RT}{v} \tag{8}$$

The number of moles of gas released into the head-space during the time interval $(t, t + \Delta t)$ is given by n times the number of bubbles generated per unit time. The last quantity is the integral of the nucleation rate with respect to time, and therefore

$$\Delta n = n \int_0^{\Delta t} J \, dt \tag{9}$$

The corresponding pressure increase, ΔP, is then given by

$$\Delta P = \frac{RTn}{v} \int_0^{\Delta t} J \, dt \tag{10}$$

so that

$$\frac{\Delta P}{\Delta t} = \left[\frac{RTn}{v}\right] J \tag{11}$$

showing that the rate of pressure rise is proportional to the rate of nucleation.

5. Discussion and conclusions

5.1. *Nucleation versus detachment*

It is plain that conventional heterogeneous nucleation theory when applied to the formation of bubbles on surfaces, whether by boiling or by growth from supersaturated gas solutions or by electrogeneration, will only be applicable to cases where the detachment process is rapid compared to the rate of nucleation. In the case of boiling some of the problems have been discussed by Cole [11], in particular the question of bubbles being trappped at the mouth of cavities (an example of so-called Harvey nuclei) and the effects this may have on the superheat limit. Cole does not explicitly discuss the problem of detachment.

Taking two possible extremes: if θ is zero and the solution perfectly wets the substrate, then detachment is effectively instantaneous, since the bubble is actually formed in the liquid phase, and the overall rate is determined solely by the nucleation kinetics. However, the nucleation rate is now that corresponding to homogeneous nucleation, and as Wilt [1] shows, for the CO_2/H_2O system at least, no homogeneous nucleation would be expected at the supersaturations used in these experiments. In two of the cases discussed in this paper the contact angle was approaching zero and yet the evolution of the CO_2 bubbles was rapid. The most probable explanation is that the nucleation sites are actually composite in nature, and may well have hydrophobic ($\theta > 0$) and hydrophilic ($\theta \simeq 0$) parts. In this way, nucleation may be facile at the same time as detachment is rapid.

The second extreme is where the contact angle approaches 180°. There are no known instances in the literature where θ actually reaches 180°, and thus this case is of no practical significance. For a hypothetical contact angle of 180°, the nucleation rate would be greatly enhanced, and whilst we have no knowledge of the detachment rate under these conditions, it is expected that this will decrease with increasing θ. There is a further consideration in the case where the contact angle is greater than 90°. Under these conditions it is likely that the bubble, upon detachment, may leave behind a significant portion of attached gas, thus causing an effective blocking of the nucleation site (forming a Harvey nucleus at the same time). Indeed, this remaining attached gas may be present with contact angles below 90°. The analogy with the pendent drop of liquid is close, where the simplest model, in which the gravitational force is conceptually balanced by the action of surface tension around the drop foot is used to calculate the detaching drop volume is inaccurate because of the amount of liquid retained on the solid surface when the drop detaches. The amount of fluid remaining attached to the substrate can be calculated, as shown in [12].

We can define a dimensionless number, $\mathscr{L}$, as the ratio of the time τ_d, required for the detachment of a bubble, and the time, τ_n, required for the nucleation event. If $\mathscr{L} = \tau_d/\tau_n < 1$, then nucleation is the rate-determining step in the overall kinetics, whilst if $\mathscr{L} > 1$, then the detachment is kinetically dominant.

The experiments on the CR39 treated with chlorotrimethyl silane have contact angles in the range expected to give large τ_d, and so large $\mathscr{L}$. It is not surprising that experimental results show the kinetics to be governed by detachment in this system.

5.2. *Nucleation kinetics*

In the region where $\mathscr{L} < 1$, and the kinetics are dominated by the nucleation rate, Equation 7 is found to describe the data well. It should be noted that the exact magnitude of the pre-exponential factor, B', is not important in determining the fit of Equation 7, since ln J has been plotted against $(\sigma P)^{-2}$, and any variation in B' will therefore only appear as an offset of the curve.

5.3. *The acoustic method*

It will be noted that when bubbles detach easily, then the rate of nucleation is closely correlated with the rate of bubble bursting at the free liquid surface. This is not true when the detachment is kinetically important, since the bubbles remain attached at the nucleation sites, and further nucleation is prevented. A condition for the acoustic method to be useful is therefore that $\mathscr{L} < 1$. This is not as severe a restriction as it might at first seem, since in many situations met in practice,

the contact angle is zero, or near zero, and the condition $\mathscr{L} < 1$ will then be fulfilled. The value of $\mathscr{L}$ is sensitive to the value of J, and it may therefore be possible to alter conditions to make $\mathscr{L} < 1$, at least when the system is in a region close to $\mathscr{L} = 1$. This may have practical implications for the 'fobbing' of carbonated drinks and for electrolytic bubble nucleation.

Acknowledgement

The support of Cadbury Schweppes plc by way of a grant for the building of the apparatus is gratefully acknowledged. I would also like to thank Rob Chatfield and Dennis Henshaw for their assistance with the CR39.

References

[1] P. M. Wilt, *J. Coll. Int. Sci.* **112** (1986) 530.
[2] M. Blander and J. L. Katz, *A. I. Ch. E. J.* **21** (1975) 836.
[3] C. A. Ward, A. Balakrishnan and F. C. Hooper, *J. Basic. Eng.* **85** (1970) 695.
[4] C. A. Ward, P. Tikuisis and R. D. Venter, *J. Appl. Phys.* **53** (1982) 6076.
[5] L. N. Tao, *J. Chem. Phys.* **69** (1974) 4189.
[6] See, for example, A. Findlay and G. King, *J. Chem. Soc. Trans.* **103** (1913) 1170.
[7] S. D. Lubetkin and M. R. Blackwell, *J. Coll. Int. Sci.* **126** (1988) 610.
[8] S. D. Lubetkin and W. J. Dunning, *J. Crystal Growth* **67** (1984) 528.
[9] A. P. Fews and D. L. Henshaw, *Nucl. Instr. Meth.* **197** (1982) 517; see also T. Portwood, D. L. Henshaw and J. Stejny, *J. Nucl. Tracks* **12** (1986) 109.
[10] S. C. Curran and J. D. Craggs 'Counting Tubes – Theory and Applications', Butterworths, London (1949) p. 95.
[11] R. Cole, *Adv. Heat Transfer* **10** (1974) 85.
[12] E. A. Boucher and H. J. Kent, *J. Coll. Int. Sci.* **67** (1978) 10.